

PREPARATION AND OPERATIONS OF THE MISSION PERFORMANCE
CENTRE (MPC) FOR THE COPERNICUS SENTINEL-3 MISSION

S3-A SLSTR Cyclic Performance Report

Cycle No. 022

Start date: 03/09/2017

End date: 30/09/2017



*Mission
Performance
Centre*



Ref.: S3MPC.RAL.PR.02-022
Issue: 1.1
Date: 09/11/2017
Contract: 400011836/14/I-LG

Customer: ESA	Document Ref.: S3MPC.RAL.PR.02-022
Contract No.: 4000111836/14/I-LG	Date: 09/11/2017
	Issue: 1.1

Project:	PREPARATION AND OPERATIONS OF THE MISSION PERFORMANCE CENTRE (MPC) FOR THE COPERNICUS SENTINEL-3 MISSION		
Title:	S3-A SLSTR Cyclic Performance Report		
Author(s):	SLSTR ESLs		
Approved by:	D. Smith, SLSTR ESL Coordinator	Authorized by	Frédéric Rouffi, OPT Technical Performance Manager
Distribution:	ESA, EUMETSAT, S3MPC consortium		
Accepted by ESA	S. Dransfeld, MPC Deputy TO for OPT P. Féménias, MPC TO		
Filename	S3MPC.RAL.PR.02-022 - i1r1 - SLSTR Cyclic Report 022.docx		

Disclaimer

The work performed in the frame of this contract is carried out with funding by the European Union. The views expressed herein can in no way be taken to reflect the official opinion of either the European Union or the European Space Agency.





Sentinel-3 MPC
S3-A SLSTR Cyclic Performance Report
Cycle No. 022

Ref.: S3MPC.RAL.PR.02-022
 Issue: 1.1
 Date: 09/11/2017
 Page: iii

Changes Log

Version	Date	Changes
1.0	11/10/2017	First Version
1.1	09/11/2017	Event occurred on 13 th September added

List of Changes

Version	Section	Answers to RID	Changes
1.1	4		Added details of missing data on 13 th September



Table of content

1 INSTRUMENT MONITORING 1

1.1 INSTRUMENT TEMPERATURES..... 1

1.2 SCANNER PERFORMANCE 5

1.3 DETECTOR NOISE LEVELS 7

 1.3.1 VIS and SWIR channel signal-to-noise 7

 1.3.2 TIR channel NEDT 9

1.4 CALIBRATION FACTORS 11

 1.4.1 VIS and SWIR VISCAL signal response..... 11

2 LEVEL 2 SST VALIDATION13

2.1 DEPENDENCE ON LATITUDE, TCWV, SATELLITE ZA AND DATE 13

2.2 SPATIAL DISTRIBUTION OF MATCH-UPS..... 14

2.3 MATCH-UPS STATISTICS 15

3 LEVEL 2 LST VALIDATION16

3.1 CATEGORY-A VALIDATION 16

3.2 CATEGORY-C VALIDATION 18

4 EVENTS19

5 APPENDIX A20

List of Figures

Figure 1: Detector temperatures for each channel from 1st March 2016. Discontinuities occur for the infrared channels where the FPA was heated for decontamination or following an anomaly. The vertical dashed lines indicate the start and end of each cycle. ----- 1

Figure 2: Blackbody temperature and baseplate gradient trends. The vertical dashed lines indicate the start and end of each cycle. ----- 2

Figure 3: Baffle temperature trends. The vertical dashed lines indicate the start and end of each cycle. - 3

Figure 4: Opto-Mechanical Enclosure (OME) temperature trends showing the paraboloid stops and flip baffle (top two plots) and optical bench and scanner and flip assembly (lower two plots). The top two plots only show data starting from 30th July 2016. The vertical dashed lines indicate the start and end of each cycle. ----- 4

Figure 5: Scanner and flip jitter, showing mean, stddev and max/min position compared to the expected one for the nadir view. The vertical dashed lines indicate the start and end of each cycle. ----- 5

Figure 6: Scanner and flip jitter, showing mean, stddev and max/min position compared to the expected one for the oblique view. The vertical dashed lines indicate the start and end of each cycle. ----- 6

Figure 7: VIS and SWIR channel signal-to-noise of the measured VISCAL signal in each orbit. Different colours indicate different detectors. ----- 8

Figure 8: NEDT trend for the thermal channels. Blue points were calculated from the cold blackbody signal and red points from the hot blackbody. Horizontal lines indicate the requirement (dashed) and goal (dotted) as well as the measured values on ground (red and blue dashed). ----- 9

Figure 9: VISCAL signal trend for VIS channels (nadir view). -----11

Figure 10: VISCAL signal trend for SWIR channels (nadir view).-----12

Figure 11: Dependence of median and robust standard deviation of match-ups between SLSTR SST_{skin} and drifting buoy SST_{depth} for Cycle 22 as a function of latitude, total column water vapour (TCWV), satellite zenith angle and date.-----13

Figure 12: Spatial distribution of match-ups between SLSTR SST_{skin} and drifting buoy SST_{depth} for Cycle 22.14

Figure 13: Validation of the SL_2_LST product over the mid-July to mid-November reprocessed period at three Gold Standard in situ stations managed by the Karlsruhe Institute of Technology: Evora, Portugal (left); Gobabeb, Namibia (centre); Kalahari-Heimat, Namibia (right). [Results courtesy of Maria Martin through the GlobTemperature Project]-----16

Figure 14: Validation of the SL_2_LST product over the mid-July to mid-November reprocessed period at the seven Gold Standard in situ stations of the SURFRAD network plus a Gold Standard station from the ARM network: Bondville, Illinois top-(left); Desert Rock, Nevada (top-centre); Fort Peck, Montana (top-right); Goodwin Creek, Mississippi (middle-left); Penn State University, Pennsylvania (middle-centre); Sioux Fall, South Dakota (middle-right); Table Mountain, Colorado (bottom-left); and Southern Great Plains, Oklahoma (bottom-centre). -----17

Figure 15: Level-1 image for channel S8 nadir view on 13th September 2017 from 08:17 to 08:20. -----19

Figure 16: Level-1 image for channel S7 nadir view on 25th September 2017 from 14:26 to 14:29, showing the gap due to missing data. -----19

List of Tables

Table 1: Average reflectance factor, and signal-to-noise ratio of the measured VISCAL signal for cycles 011-022, averaged over all detectors for the nadir view. ----- 7

Table 2: Average reflectance factor, and signal-to-noise ratio of the measured VISCAL signal for cycles 011-022, averaged over all detectors for the oblique view. ----- 7

Table 3: NEDT for cycles 011-022 averaged over all detectors for both Earth views towards the +YBB (hot). -----10

Table 4: NEDT for cycles 011-022 averaged over all detectors for both Earth views towards the -YBB (cold). -----10

Table 5: SLSTR drifter match-up statistics for Cycle 22. -----15



1 Instrument monitoring

1.1 Instrument temperatures

- ❖ Instrument temperatures were stable and consistent with expected values following the decontamination phase which was performed towards the end of Cycle 20.
- ❖ Blackbody, baffle and OME temperatures peaked at the beginning of the year when the Earth was at perihelion. In Cycle 22, the blackbody temperatures were at their expected values, just beginning to rise as we approach the end of the year. Gradients across the blackbody baseplate are stable and within their expected range.

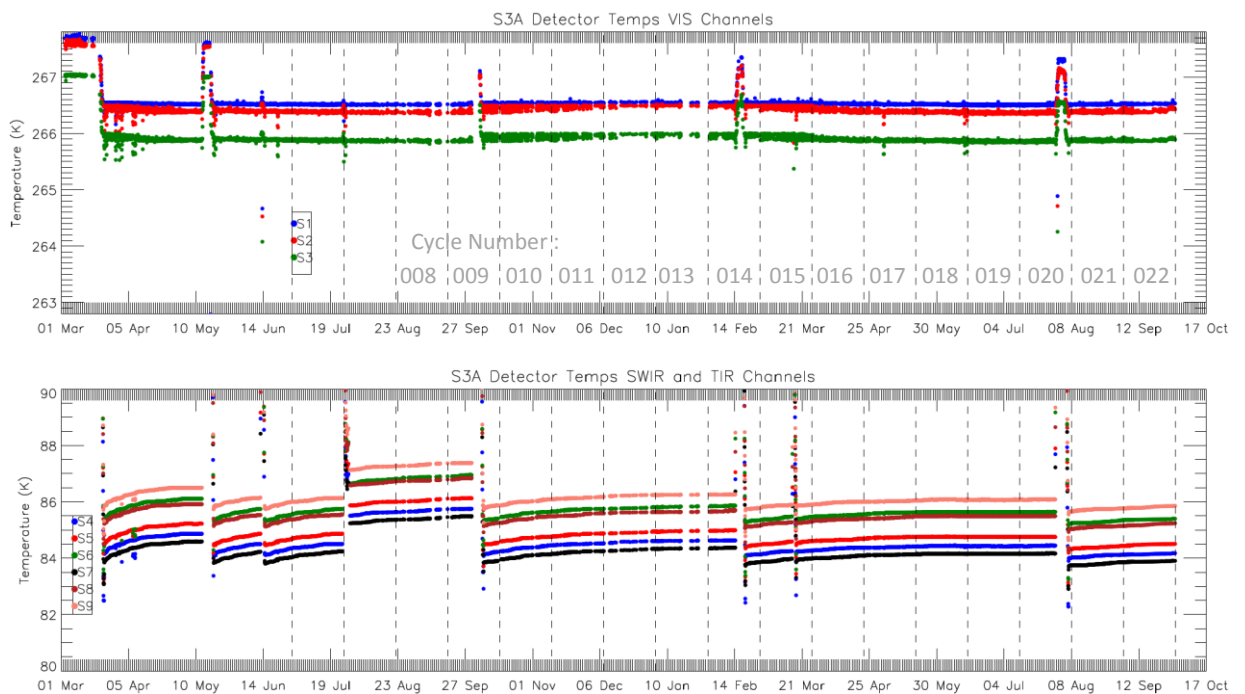


Figure 1: Detector temperatures for each channel from 1st March 2016. Discontinuities occur for the infrared channels where the FPA was heated for decontamination or following an anomaly. The vertical dashed lines indicate the start and end of each cycle.



Sentinel-3 MPC
S3-A SLSTR Cyclic Performance Report
Cycle No. 022

Ref.: S3MPC.RAL.PR.02-022
Issue: 1.1
Date: 09/11/2017
Page: 2

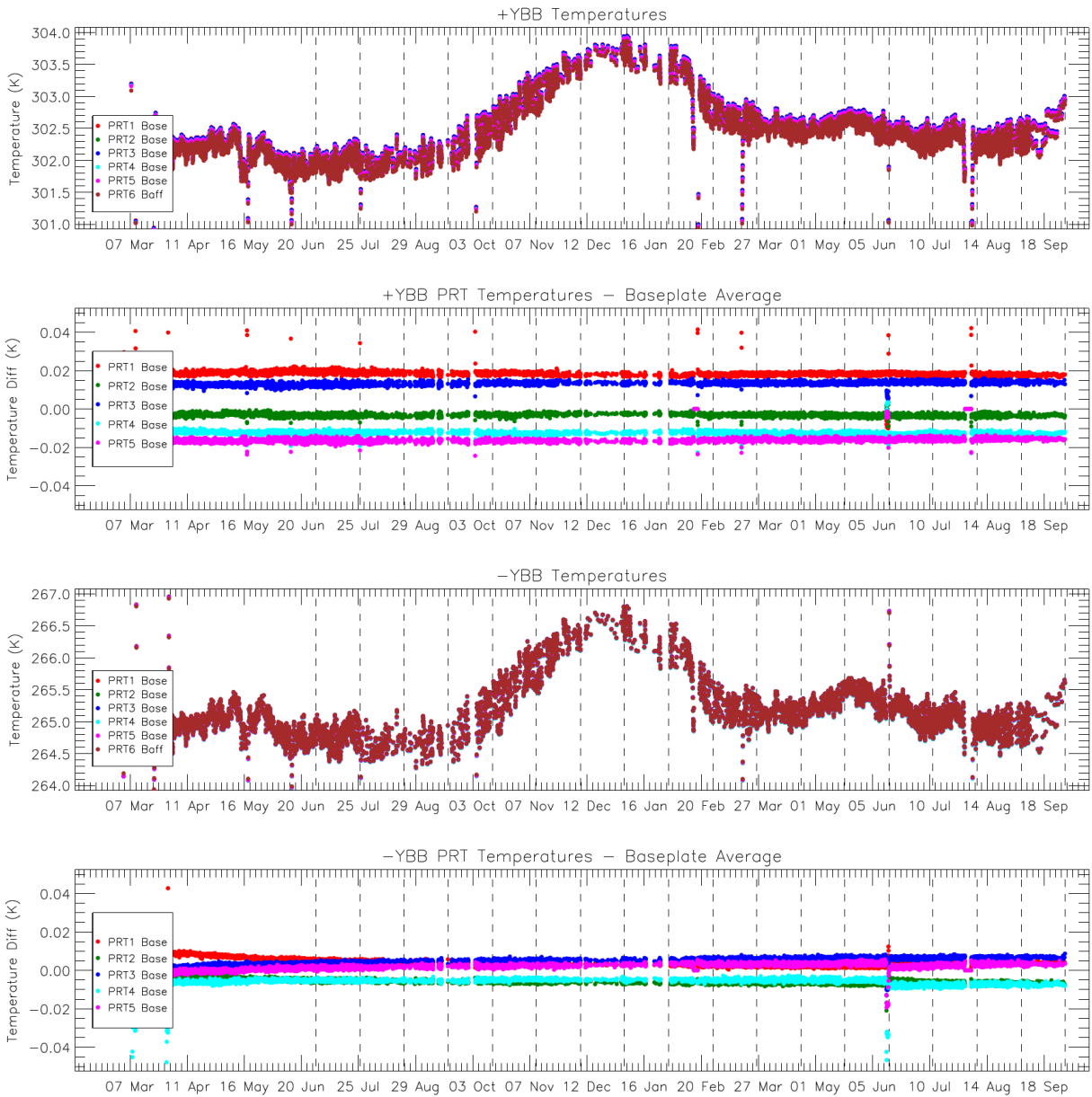


Figure 2: Blackbody temperature and baseplate gradient trends. The vertical dashed lines indicate the start and end of each cycle.



Sentinel-3 MPC
S3-A SLSTR Cyclic Performance Report
Cycle No. 022

Ref.: S3MPC.RAL.PR.02-022
Issue: 1.1
Date: 09/11/2017
Page: 3

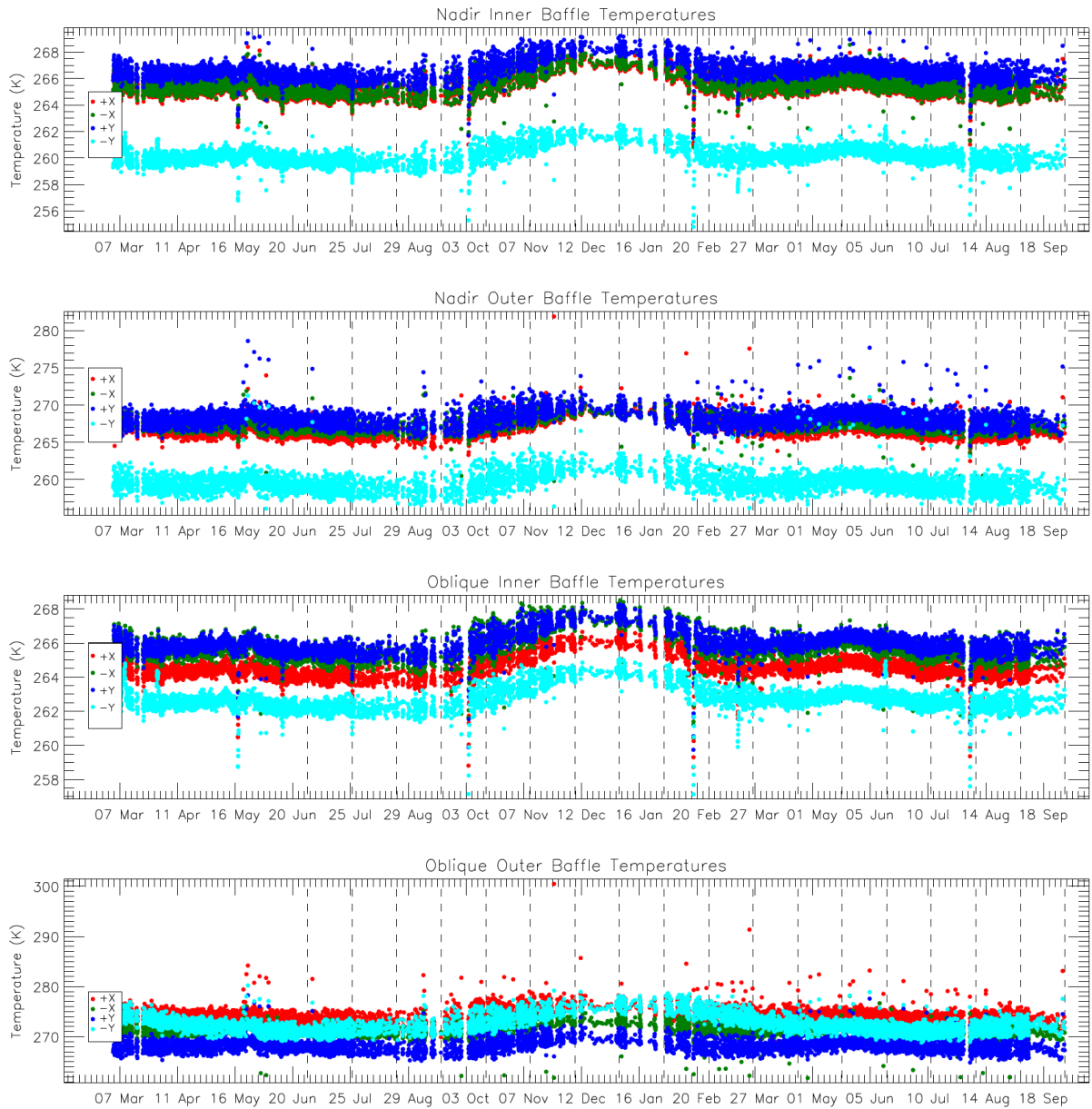


Figure 3: Baffle temperature trends. The vertical dashed lines indicate the start and end of each cycle.



Sentinel-3 MPC
S3-A SLSTR Cyclic Performance Report
Cycle No. 022

Ref.: S3MPC.RAL.PR.02-022
Issue: 1.1
Date: 09/11/2017
Page: 4

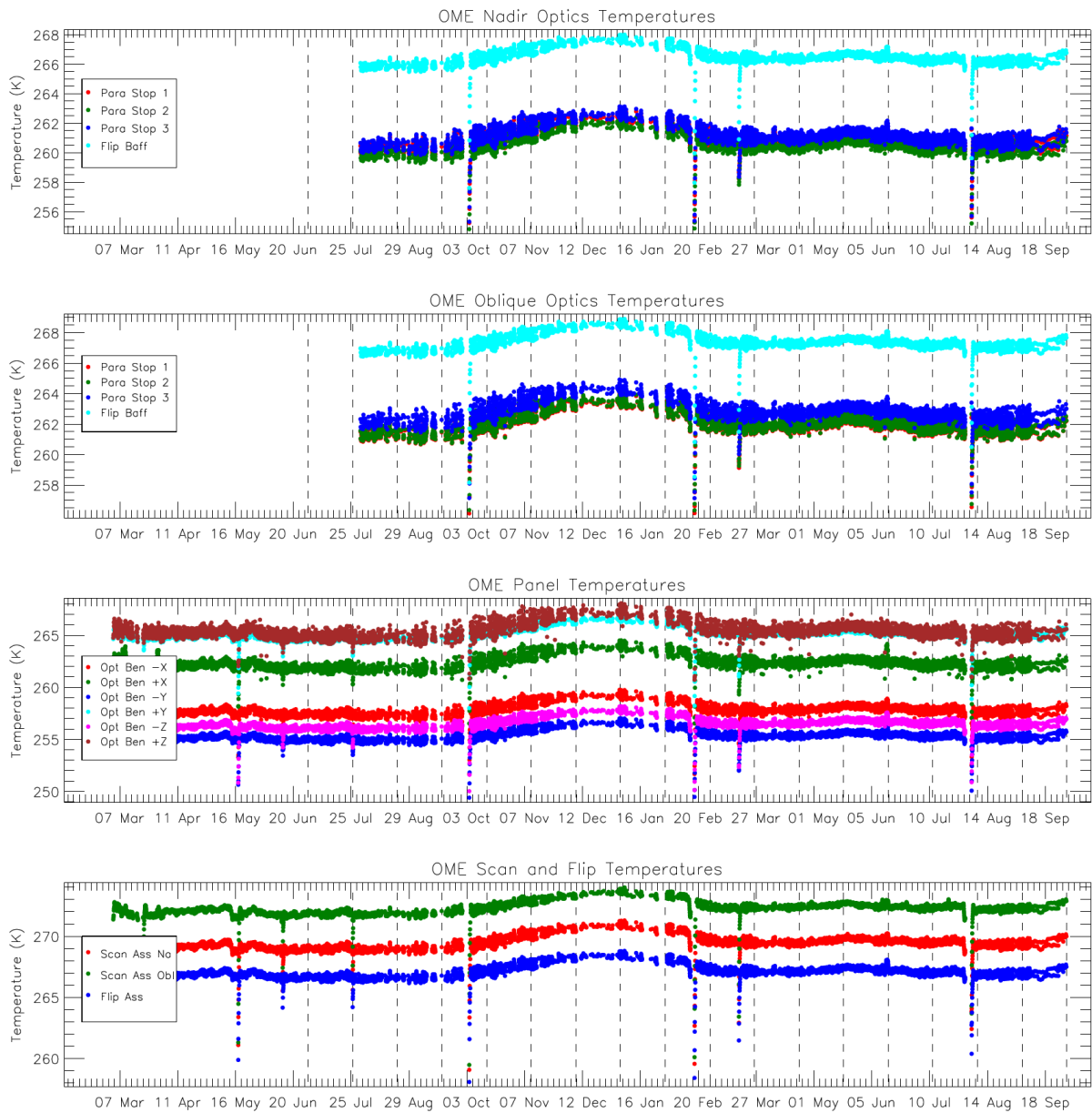


Figure 4: Opto-Mechanical Enclosure (OME) temperature trends showing the paraboloid stops and flip baffle (top two plots) and optical bench and scanner and flip assembly (lower two plots). The top two plots only show data starting from 30th July 2016. The vertical dashed lines indicate the start and end of each cycle.



1.2 Scanner performance

Scanner performance has been consistent with previous operations and within required limits.

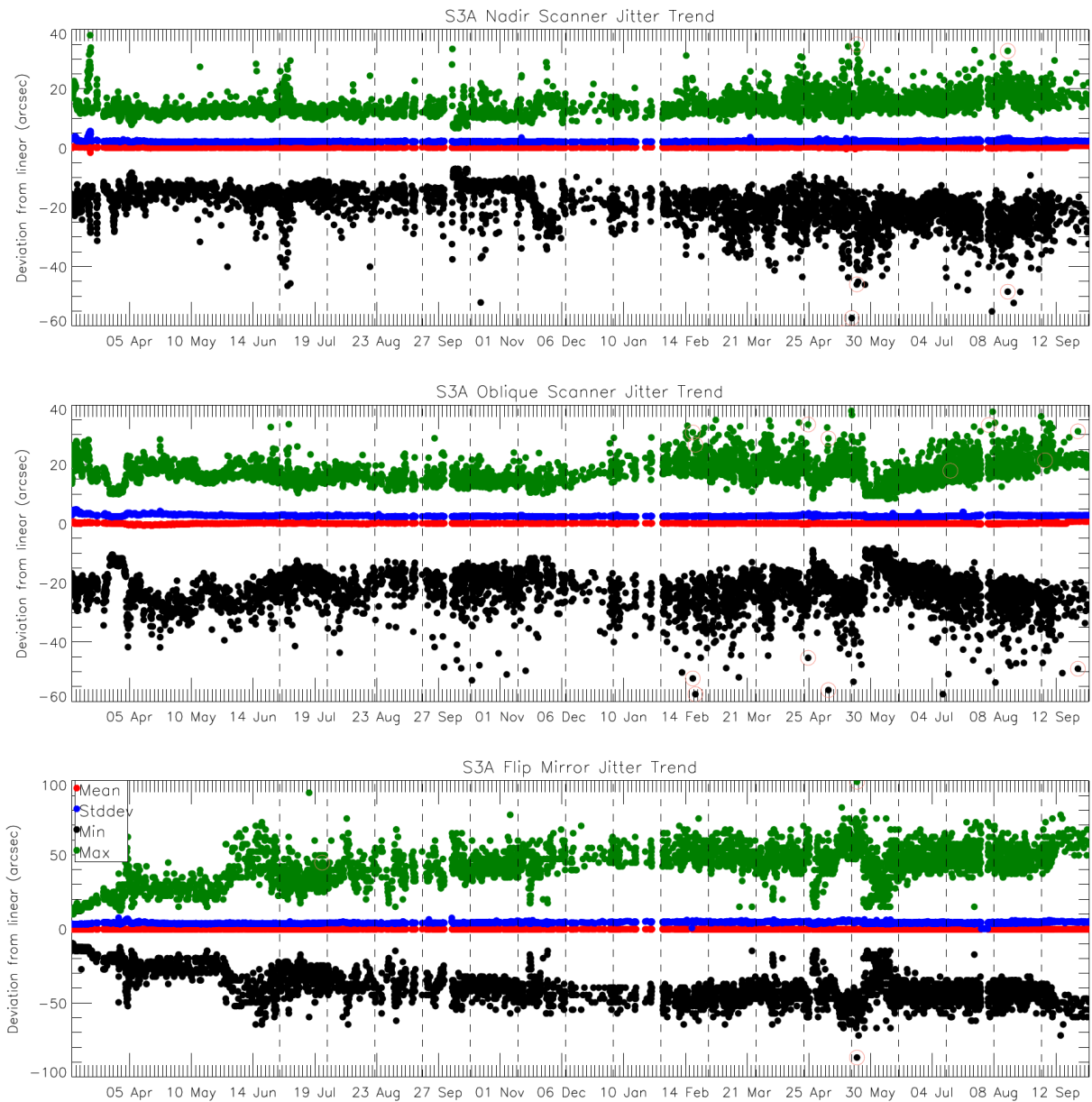


Figure 5: Scanner and flip jitter, showing mean, stddev and max/min position compared to the expected one for the nadir view. The vertical dashed lines indicate the start and end of each cycle.

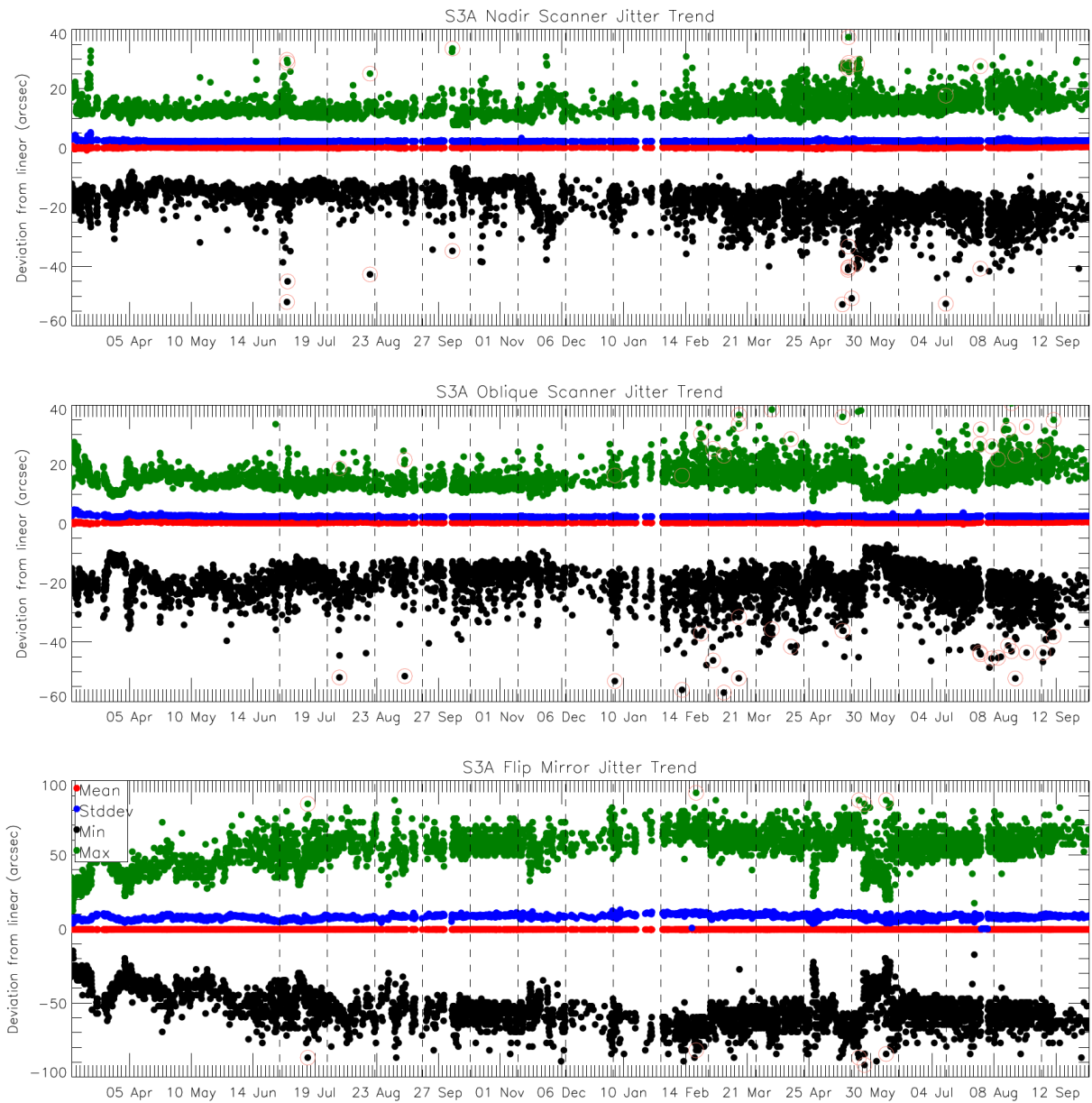


Figure 6: Scanner and flip jitter, showing mean, stddev and max/min position compared to the expected one for the oblique view. The vertical dashed lines indicate the start and end of each cycle.



1.3 Detector noise levels

1.3.1 VIS and SWIR channel signal-to-noise

The VIS and SWIR channel noise was stable and consistent with previous operations - the signal-to-noise ratio of the measured VISCAL signal is plotted in Figure 7. Table 1 and Table 2 give the average signal-to-noise in each cycle (excluding the anomaly/decontamination period in Cycle 20). Note that this averages over the significant detector-detector dispersion for the SWIR channels that is shown in Figure 7.

Table 1: Average reflectance factor, and signal-to-noise ratio of the measured VISCAL signal for cycles 011-022, averaged over all detectors for the nadir view.

	Average Reflectance Factor	Nadir Signal-to-noise ratio											
		Cycle 011	Cycle 012	Cycle 013	Cycle 014	Cycle 015	Cycle 016	Cycle 017	Cycle 018	Cycle 019	Cycle 020	Cycle 021	Cycle 022
S1	0.187	235	233	226	217	224	233	234	231	229	233	231	231
S2	0.194	238	236	234	227	230	236	236	232	231	235	235	234
S3	0.190	239	235	230	221	230	236	238	228	231	230	229	228
S4	0.191	145	141	139	137	139	142	140	140	139	137	135	135
S5	0.193	235	238	234	234	233	233	235	236	233	232	232	230
S6	0.175	147	145	143	141	144	142	143	143	142	140	136	139

Table 2: Average reflectance factor, and signal-to-noise ratio of the measured VISCAL signal for cycles 011-022, averaged over all detectors for the oblique view.

	Average Reflectance Factor	Oblique Signal-to-noise ratio											
		Cycle 011	Cycle 012	Cycle 013	Cycle 014	Cycle 015	Cycle 016	Cycle 017	Cycle 018	Cycle 019	Cycle 020	Cycle 021	Cycle 022
S1	0.166	249	247	238	229	236	243	247	246	242	241	241	243
S2	0.170	253	250	241	232	241	248	251	249	247	247	244	244
S3	0.168	251	244	237	227	236	245	249	244	242	239	234	240
S4	0.166	112	112	108	107	108	108	111	110	109	108	108	108
S5	0.166	173	173	169	169	172	169	169	171	168	168	168	168
S6	0.155	114	113	105	106	107	109	109	110	108	106	108	107



Sentinel-3 MPC

S3-A SLSTR Cyclic Performance Report

Cycle No. 022

Ref.: S3MPC.RAL.PR.02-022

Issue: 1.1

Date: 09/11/2017

Page: 8

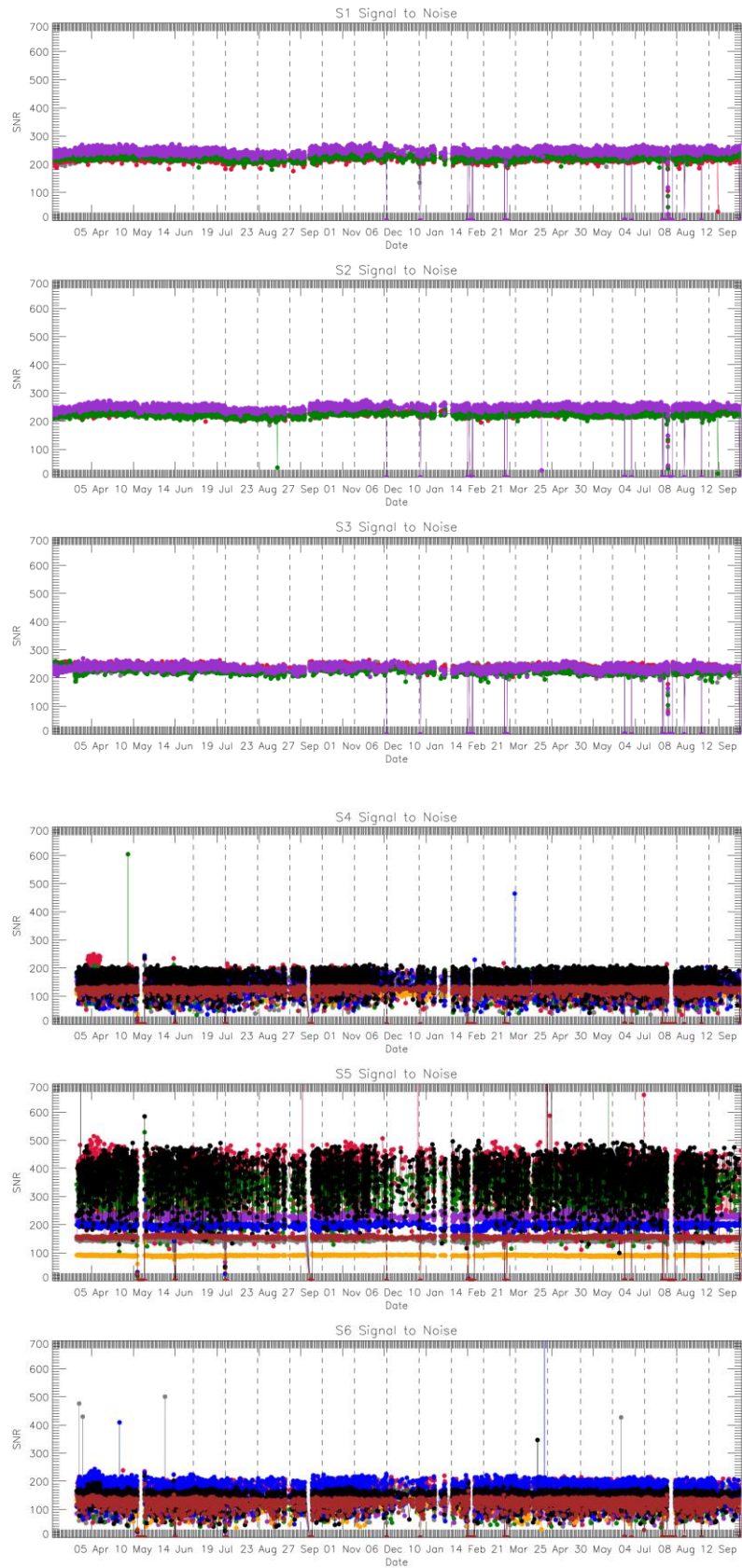


Figure 7: VIS and SWIR channel signal-to-noise of the measured VISCAL signal in each orbit. Different colours indicate different detectors.



Sentinel-3 MPC
S3-A SLSTR Cyclic Performance Report
Cycle No. 022

Ref.: S3MPC.RAL.PR.02-022
Issue: 1.1
Date: 09/11/2017
Page: 9

1.3.2 TIR channel NEDT

The thermal channel NEDT values are consistent with previous operations and within the requirements. NEDT values for each cycle, averaged over all detectors and both Earth views, are shown in Table 3 and Table 4.

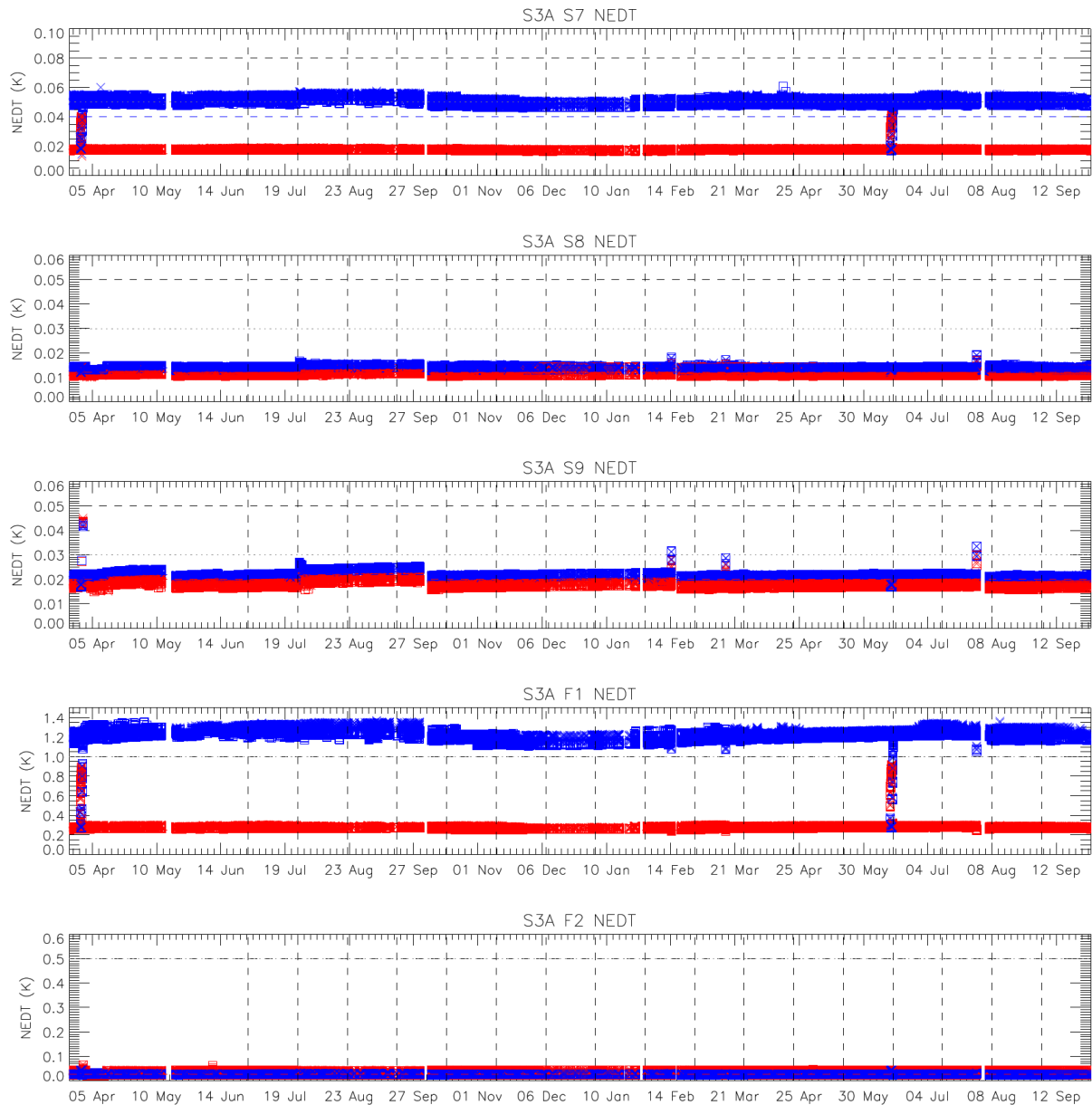


Figure 8: NEDT trend for the thermal channels. Blue points were calculated from the cold blackbody signal and red points from the hot blackbody. Horizontal lines indicate the requirement (dashed) and goal (dotted) as well as the measured values on ground (red and blue dashed).



Sentinel-3 MPC

S3-A SLSTR Cyclic Performance Report

Cycle No. 022

Ref.: S3MPC.RAL.PR.02-022
 Issue: 1.1
 Date: 09/11/2017
 Page: 10

Table 3: NEDT for cycles 011-022 averaged over all detectors for both Earth views towards the +YBB (hot).

	Cycle 011	Cycle 012	Cycle 013	Cycle 014	Cycle 015	Cycle 016	Cycle 017	Cycle 018	Cycle 019	Cycle 020	Cycle 021	Cycle 022
+YBB temp (K)	303.289	303.680	303.621	303.206	302.674	302.544	302.541	302.593	302.386	302.348	302.307	302.479
NEDT (mK)												
S7	16.9	16.9	16.8	16.9	17.2	17.2	17.2	18.1	17.2	17.2	17.1	17.2
S8	11.0	11.0	11.1	11.0	10.9	10.9	11.0	11.1	11.0	11.1	10.9	10.9
S9	17.4	17.7	17.9	17.6	17.0	17.0	17.2	17.5	17.4	17.5	16.7	16.9
F1	260	260	260	260	268	268	271	297	276	276	269	270
F2	27.7	28.0	28.0	27.9	27.6	27.6	27.8	27.8	27.8	27.8	27.3	27.6

Table 4: NEDT for cycles 011-022 averaged over all detectors for both Earth views towards the -YBB (cold).

	Cycle 011	Cycle 012	Cycle 013	Cycle 014	Cycle 015	Cycle 016	Cycle 017	Cycle 018	Cycle 019	Cycle 020	Cycle 021	Cycle 022
-YBB temp (K)	266.112	266.512	266.353	265.807	265.183	265.136	265.260	265.412	265.125	265.000	264.902	265.032
NEDT (mK)												
S7	47.2	46.6	46.8	47.9	48.7	49.0	48.8	46.9	49.1	49.5	49.5	49.0
S8	14.4	14.5	14.4	14.4	14.2	14.2	14.3	14.2	14.3	14.4	14.2	14.1
S9	21.8	22.2	22.4	22.1	21.3	21.4	21.6	21.6	21.9	22.0	21.1	21.3
F1	1162	1123	1130	1178	1222	1191	1199	1163	1229	1235	1212	1201
F2	29.5	29.6	29.6	29.6	29.2	29.3	29.3	29.4	29.6	29.7	29.2	29.2



1.4 Calibration factors

1.4.1 VIS and SWIR VISCAL signal response

Signals from the VISCAL source for the VIS channels show oscillations due to the build up of ice on the optical path within the FPA. Decontamination must be carried out periodically in order to warm up the FPA and remove the ice. The latest decontamination cycle was successfully performed at the end of Cycle 20. The VISCAL signal has behaved as expected following the decontamination.

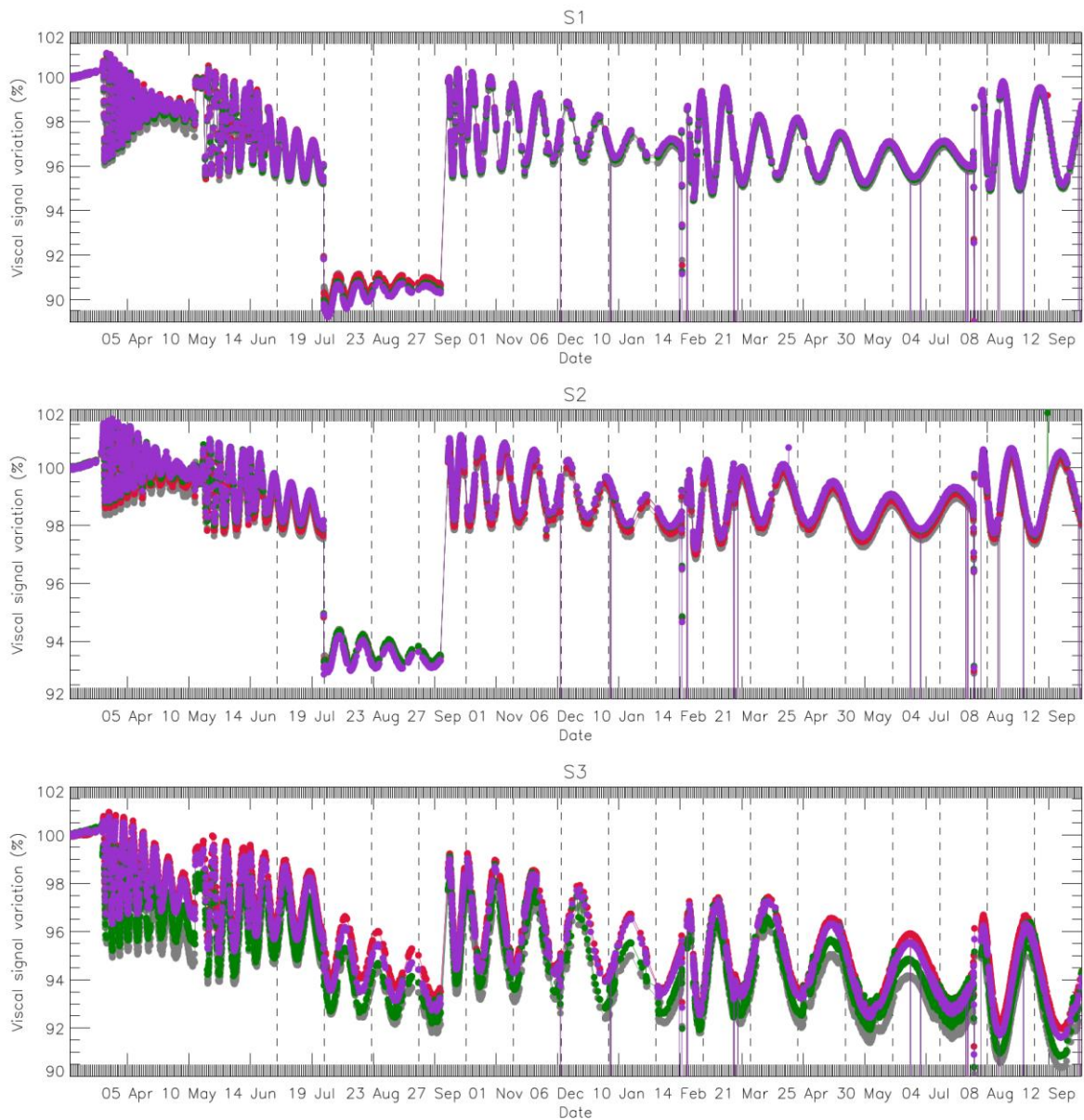


Figure 9: VISCAL signal trend for VIS channels (nadir view).

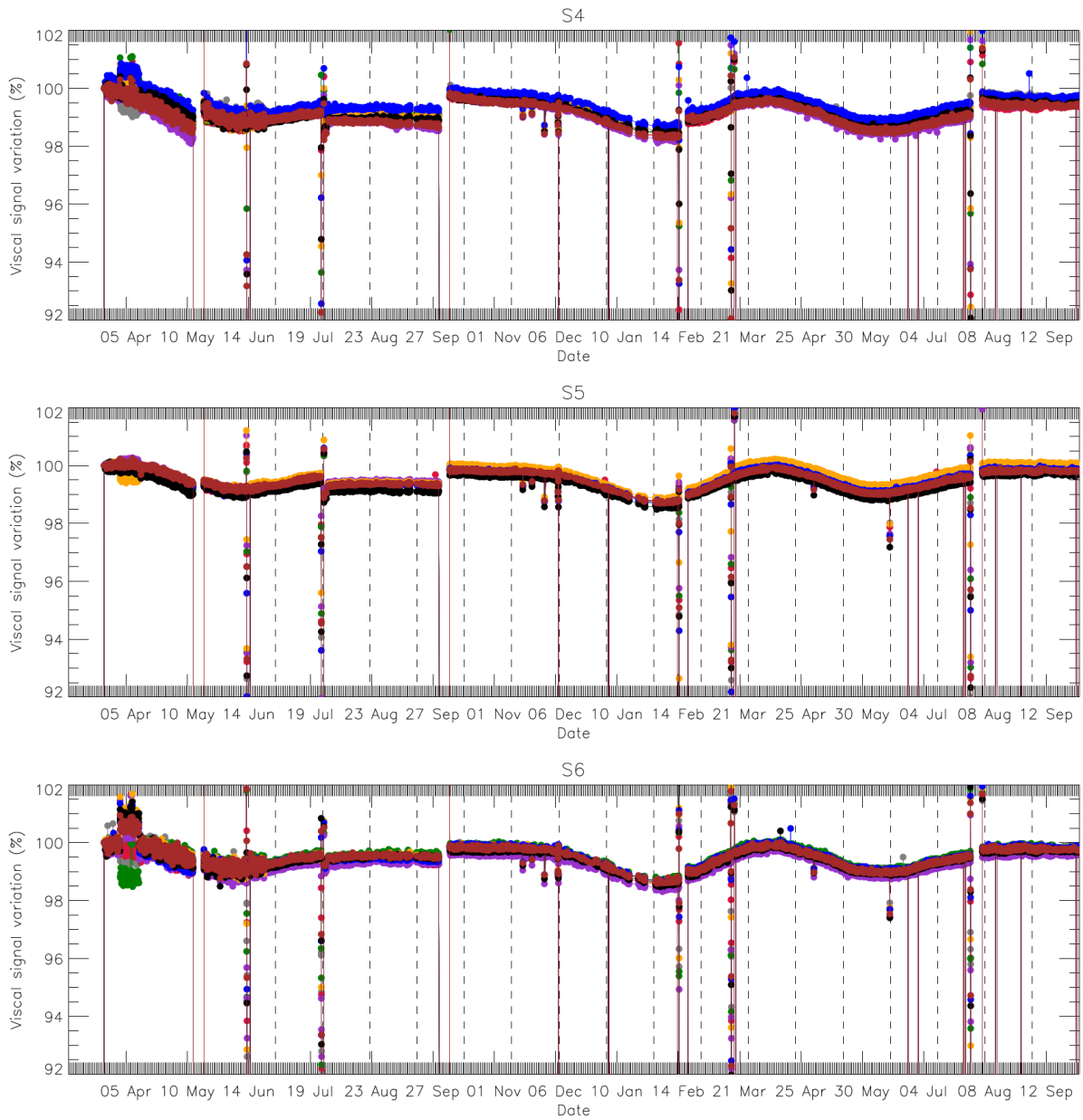


Figure 10: VISCAL signal trend for SWIR channels (nadir view).



2 Level 2 SST validation

Level 2 WCT SSTs have been validated using CMEMS *in situ* data for Cycle 22. Match-ups between SLSTR and *in situ* data are provided by the EUMESAT OSI-SAF.

2.1 Dependence on latitude, TCWV, Satellite ZA and date

- ❖ The dependence of the difference between SLSTR SST_{skin} and drifting buoy SST_{depth} is shown in Figure 11. No adjustments have been made for difference in depth or time between the satellite and *in situ* measurements. SLSTR SSTs are extracted from the SL_2_WCT files. Daytime 2-channel (S8 and S9) results are shown in red, night time 2-channel results are shown in blue and night time 3-channel results are shown in green. Solid lines indicate dual-view retrievals, dashed lines indicate nadir-only retrievals. Bold lines indicate statistically significant (95% confidence) results.

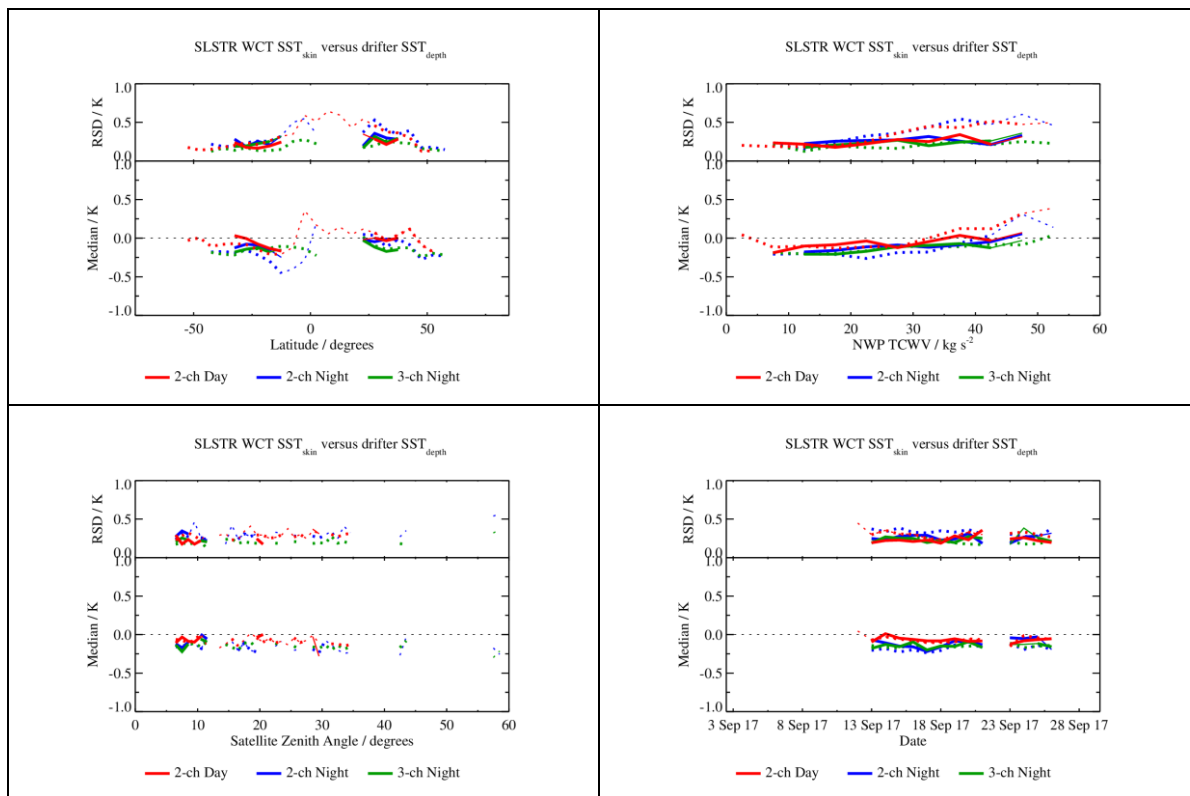


Figure 11: Dependence of median and robust standard deviation of match-ups between SLSTR SST_{skin} and drifting buoy SST_{depth} for Cycle 22 as a function of latitude, total column water vapour (TCWV), satellite zenith angle and date.



2.2 Spatial distribution of match-ups

- ❖ The spatial distribution of SLSTR/drifter match-ups for Cycle 22 is shown in Figure 12. No adjustments have been made for difference in depth or time between the satellite and *in situ* measurements.

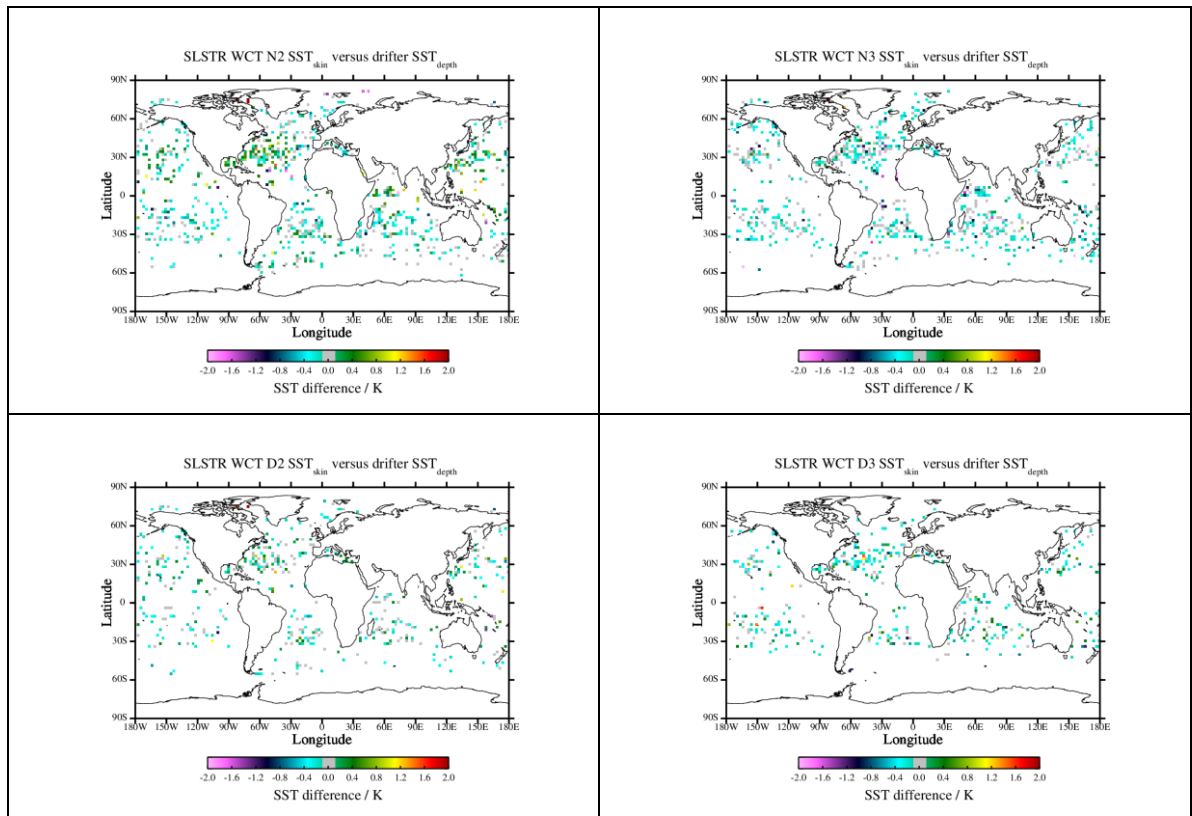


Figure 12: Spatial distribution of match-ups between SLSTR SST_{skin} and drifting buoy SST_{depth} for Cycle 22.



2.3 Match-ups statistics

- ❖ Match-ups statistics (median and robust standard deviation, RSD) of SLSTR/drifter match-ups for Cycle 22 are shown in Table 5. No adjustments have been made for difference in depth or time between the satellite and in situ measurements and so at night time (in the absence of diurnal warming) an offset of around -0.17 K is expected. The RSD values indicate SLSTR is providing SSTs mostly within its target accuracy (0.3 K).

Table 5: SLSTR drifter match-up statistics for Cycle 22.

Retrieval	Number	Median (K)	RSD (K)
N2 day	17702	-0.07	0.30
D2 day	790	-0.07	0.24
N2 night	1803	-0.18	0.33
N3 night	1803	-0.15	0.21
D2 night	730	-0.11	0.27
D3 night	730	-0.15	0.24



3 Level 2 LST validation

Level 2 Land Surface Temperature products have been validated against *in situ* observations (Category-A validation), and intercompared (Category-C validation) with respect to three independent reference products from the ESA DUE GlobTemperature Project (MODIS, GOES, and SEVIRI).

3.1 Category-A validation

Category-A validation uses a comparison of satellite-retrieved LST with *in situ* measurements collected from radiometers sited at a number of stations spread across the Earth, for which the highest-quality validation can be achieved. The results can be summarised as follows (see Figure 13 and Figure 14):

- ❖ Average absolute accuracy (vs. Gold Standard):
 - Daytime: 0.81K
 - Night-time: 1.07K

This daytime accuracy meets the mission requirement of < 1K. The night-time accuracy is very close to this mission requirement. This also is in line with the GCOS climate requirements of 1 K accuracy.

- ❖ Average precision (vs. Gold Standard):
 - Daytime: 0.72K
 - Night-time: 1.21K

While there is no Sentinel-3 mission requirement for precision, the daytime precision meets the GCOS climate requirement of 1K. The night-time accuracy is also very close to this climate requirement.

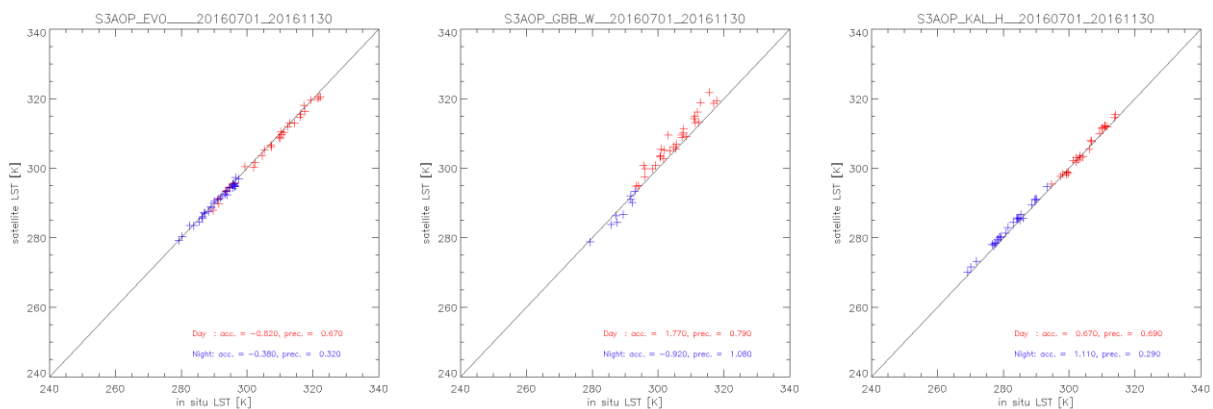


Figure 13: Validation of the SL_2_LST product over the mid-July to mid-November reprocessed period at three Gold Standard *in situ* stations managed by the Karlsruhe Institute of Technology: Evora, Portugal (left); Gobabeb, Namibia (centre); Kalahari-Heimat, Namibia (right). [Results courtesy of Maria Martin through the GlobTemperature Project]

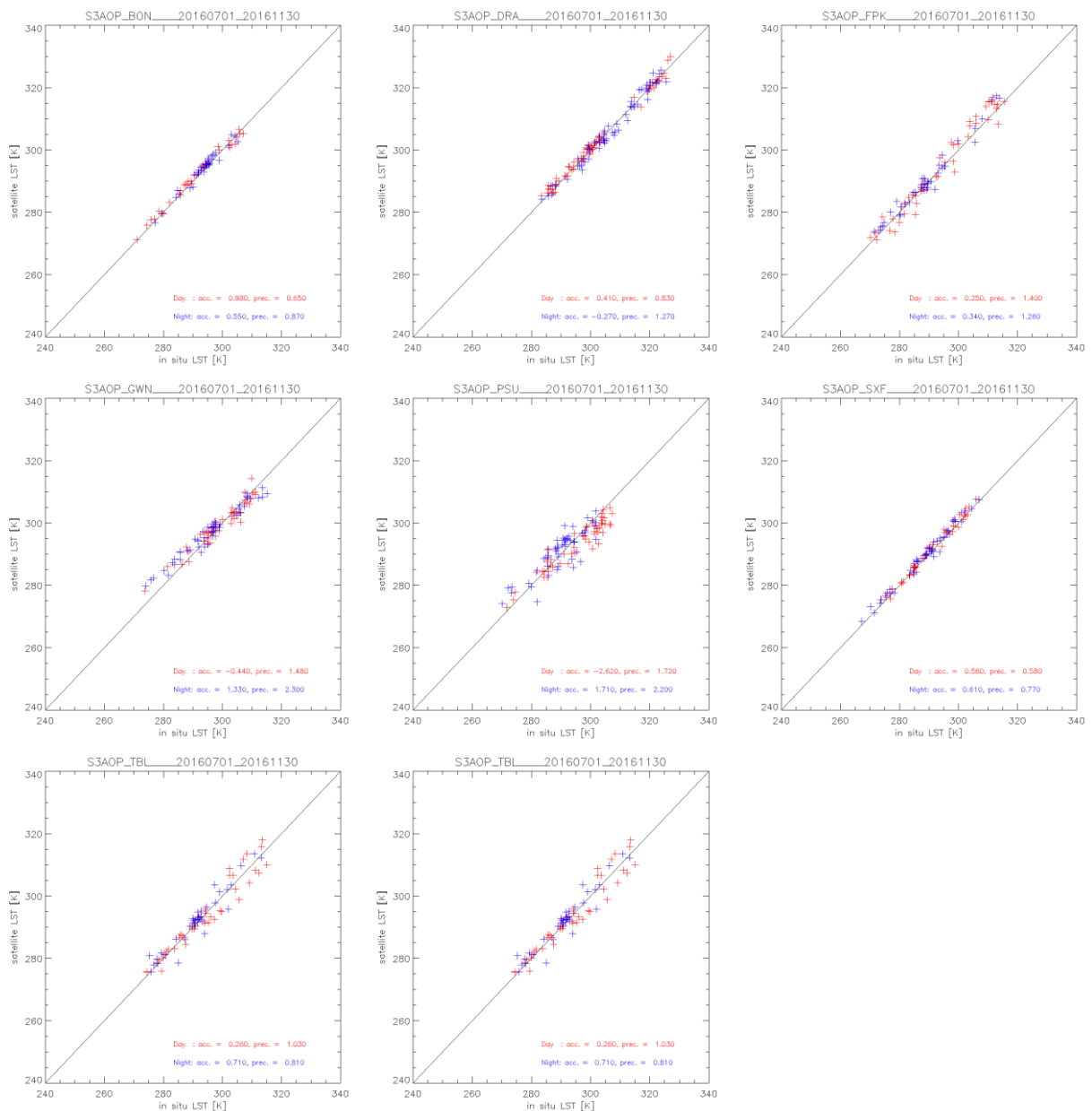



Figure 14: Validation of the SL₂LST product over the mid-July to mid-November reprocessed period at the seven Gold Standard in situ stations of the SURFRAD network plus a Gold Standard station from the ARM network: Bondville, Illinois top-(left); Desert Rock, Nevada (top-centre); Fort Peck, Montana (top-right); Goodwin Creek, Mississippi (middle-left); Penn State University, Pennsylvania (middle-centre); Sioux Fall, South Dakota (middle-right); Table Mountain, Colorado (bottom-left); and Southern Great Plains, Oklahoma (bottom-centre).

	<p>Sentinel-3 MPC</p> <p>S3-A SLSTR Cyclic Performance Report</p> <p>Cycle No. 022</p>	<p>Ref.: S3MPC.RAL.PR.02-022</p> <p>Issue: 1.1</p> <p>Date: 09/11/2017</p> <p>Page: 18</p>
--	---	--

3.2 Category-C validation

Category-C validation uses inter-comparisons with similar LST products from other sources such as AATSR, AVHRR, MODIS, SEVIRI, and VIIRS, which give important quality information with respect to spatial patterns in LST deviations. The results can be summarised as follows:

- ❖ Daytime intercomparison differences are: ~1K vs. GOES__LST_2 over North America; ~1K vs. SEVIR_LST_2 over Europe; and < 1K vs. MOGSV_LST_2 on a Global basis.
- ❖ Night-time intercomparison differences are: <1K vs. GOES__LST_2 over North America; <1K vs. SEVIR_LST_2 over Europe; and < 1K vs. MOGSV_LST_2 on a Global basis.
- ❖ Differences with respect to biomes tend to be larger during the day for surfaces with more heterogeneity and/or higher solar insolation. With respect to SLSTR zenith viewing angle differences are larger in the day on the left side of the SLSTR swath in the along-track direction.



4 Events

SLSTR was switched on and operating nominally during the cycle, with SUE scanning and autonomous switching between day and night modes. However, there were two periods which suffered from a loss of data during downlink as described below.

A short loss of data occurred during downlink to the ground station on the 13th September 2017 due to radio frequency interference with another satellite. This resulted in a series of stripes due to missing data packets in the granule from 08:17:43 to 08:20:43 (see Figure 15).

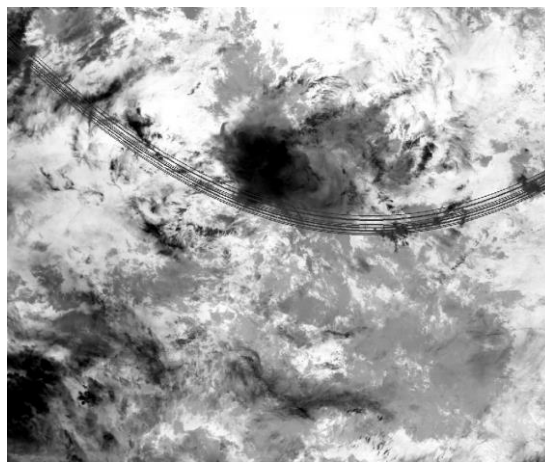


Figure 15: Level-1 image for channel S8 nadir view on 13th September 2017 from 08:17 to 08:20.

A second loss of data occurred during downlink to the ground station on the 25th September 2017 at 14:28:56. This resulted in a gap of approximately 8 seconds and therefore a band of missing data in the Level-1 and Level-2 images. Due to the calibration cycle of 20 scans for the thermal channels, the effect of the gap lasts for a further 1.5 seconds for S7-S9. The calibration of the image is unaffected following this short interruption. An example Level-1 image showing the gap is given in Figure 16.

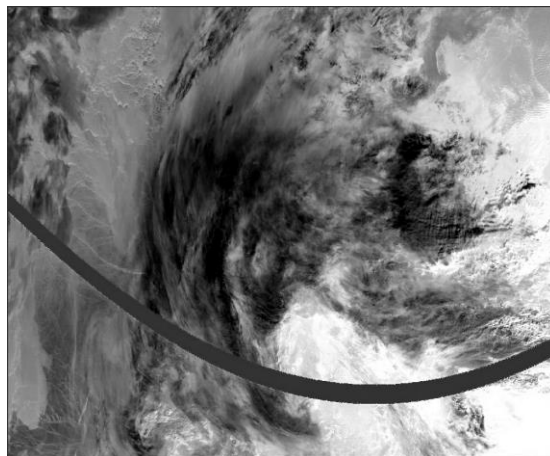



Figure 16: Level-1 image for channel S7 nadir view on 25th September 2017 from 14:26 to 14:29, showing the gap due to missing data.

 <p>SENTINEL 3 Mission Performance Centre</p>	<p>Sentinel-3 MPC</p> <p>S3-A SLSTR Cyclic Performance Report</p> <p>Cycle No. 022</p>	<p>Ref.: S3MPC.RAL.PR.02-022</p> <p>Issue: 1.1</p> <p>Date: 09/11/2017</p> <p>Page: 20</p>
---	---	--

5 Appendix A

Other reports related to the Optical mission are:

- ❖ S3-A OLCI Cyclic Performance Report, Cycle No. 022 (ref. S3MPC.ACR.PR.01-022)

All Cyclic Performance Reports are available on MPC pages in Sentinel Online website, at:
<https://sentinel.esa.int>

End of document